

---

This is an electronic reprint of the original article.  
This reprint may differ from the original in pagination and typographic detail.

Lu, Liangliang; Kujala, Pentti; Goerlandt, Floris

## A method for assessing ship operability in dynamic ice for independent navigation and escort operations

*Published in:*  
Ocean Engineering

*DOI:*  
[10.1016/j.oceaneng.2021.108830](https://doi.org/10.1016/j.oceaneng.2021.108830)

Published: 01/04/2021

*Document Version*  
Publisher's PDF, also known as Version of record

*Published under the following license:*  
CC BY-NC-ND

*Please cite the original version:*  
Lu, L., Kujala, P., & Goerlandt, F. (2021). A method for assessing ship operability in dynamic ice for independent navigation and escort operations. *Ocean Engineering*, 225, Article 108830.  
<https://doi.org/10.1016/j.oceaneng.2021.108830>

---

This material is protected by copyright and other intellectual property rights, and duplication or sale of all or part of any of the repository collections is not permitted, except that material may be duplicated by you for your research use or educational purposes in electronic or print form. You must obtain permission for any other use. Electronic or print copies may not be offered, whether for sale or otherwise to anyone who is not an authorised user.



# A method for assessing ship operability in dynamic ice for independent navigation and escort operations

Liangliang Lu<sup>a,\*</sup>, Pentti Kujala<sup>a</sup>, Floris Goerlandt<sup>b</sup>

<sup>a</sup> Aalto University, School of Engineering, Department of Mechanical Engineering, Marine Technology, P.O. Box 15300, 00076, Aalto, Finland

<sup>b</sup> Dalhousie University, Department of Industrial Engineering, Halifax, Nova Scotia, B3H 4R2, Canada

## ARTICLE INFO

### Keywords:

Ship operability  
Dynamic ice  
Ice navigation  
Independent navigation  
Icebreaker escort operation  
AIS data

## ABSTRACT

Ships navigating in ice inevitably encounter different ice conditions. Dynamic ice typically presents severe conditions when it is moving perpendicular towards the parallel midship section, which can lead to ships getting stuck in ice. This can cause delays for ships or even damage to the ship hull. However, there currently is no model to assess ship operability in this dynamic ice. This paper aims to develop a method to assess operability of ships in dynamic ice conditions, which can be used for ship routing to avoid ship stuck. The method is especially useful for emergency response planning purposes, e.g. for marine pollution preparedness and response planning, where an understanding of the operability of response vessels in dynamic ice conditions currently is lacking. First, a transit model is introduced for both independent navigation and escort operations, considering the additional ice resistance by dynamic ice. Then, a ship operability index is proposed based on the modelling of ship's performance. Case studies of independent navigation and escort operations in realistic dynamic ice conditions are investigated to compare with the simulated results. Reasonable agreement is obtained, indicating that the proposed method can be used for ship operability assessment in dynamic ice.

## 1. Introduction

Shipping in ice is a common activity in the Northern Baltic Sea during wintertime. More recently, shipping in the Arctic regions has also received increased attentions, as the projected reductions in sea ice cover due to climate change have led to an interest by shipping companies to utilize Arctic routes to reduce transit time, although associated uncertainties remain high (Beveridge et al., 2016). However, the potential of increased activities in ice expose ships to more complex and hazardous situations. While the provision of ice services such as ice forecasts is continuously developing, more specific knowledge of the ship operability for corresponding ice and environmental conditions can be beneficial for making decisions to reduce relevant risks for ships navigating in ice. For instance, Valdez Banda et al. (2016) found that further enhanced e-Navigation support e.g. through improved ship operability information can reduced the operational risks of winter navigation in a case study for the Gulf of Finland. For some emergency response situations, e.g. in marine pollution preparedness and response planning, the operability information of ships is of great importance for decision making concerning the effectiveness of the spill response system. This has been identified as a critical factor e.g. in the oil spill

response system in the Northern Baltic Sea, whereas uncertainty about this operability currently is relatively high (Lu et al. 2019, 2020). In addition, operability information in various ice conditions is important for route planning purposes, as this is essential to determine efficient and safe routes. The current route planning models in ice, e.g. Kotovirta et al. (2009), Choi et al. (2015), Montewka et al. (2019), Lehtola et al. (2019), and Zhang et al. (2019), however do not include specific features of ships in dynamic ice.

Usually, thick level ice, ridged ice and dynamic ice moving perpendicular towards the parallel midship section are considered as severe ice conditions for ships. Compared to level ice, ridged ice and dynamic ice have more factors influencing ship performance (Riska et al., 1995; Kuuliala et al., 2017), e.g. ridge size and density for ridged ice and ice drift speed for dynamic ice. Ships sailing in these conditions are subject to a relatively more hazardous situation, e.g. getting stuck in ice, due to these additional uncertain factors. However, ships besetting in thick level ice or ridged ice have the possibility to reverse and then ram into ice multiple times to break their ways, which results in a relatively low risk of getting stuck. In contrast, dynamic ice gives little chance for a ship to continue its movement as the broken channel behind the ship will close and the dynamic ice on the ship side will pose additional

\* Corresponding author.

E-mail address: [liangliang.lu@aalto.fi](mailto:liangliang.lu@aalto.fi) (L. Lu).

<https://doi.org/10.1016/j.oceaneng.2021.108830>

Received 21 September 2020; Received in revised form 20 January 2021; Accepted 28 February 2021

Available online 12 March 2021

0029-8018/© 2021 The Author(s).

Published by Elsevier Ltd.

This is an open access article under the CC BY-NC-ND license

(<http://creativecommons.org/licenses/by-nc-nd/4.0/>).

resistance. This phenomenon not only affects independent navigation, but also represents challenges to escort or convoy operations, i.e. ships following the icebreakers at a certain distance (Rosenblad, 2007). When vessels get stuck in dynamic ice, this causes delays for the ship voyage or mission, and can cause damage to the ship hull (Hänninen, 2004). Therefore, dynamic ice is generally regarded as the most challenging operational condition. It is also referred as compressive ice in other research, e.g. Riska et al. (1995), Kaups (2011), Külaots et al. (2013), and Li et al. (2019) as the moving ice will cause compression in the ice field when it hits an obstacle.

Significant research has been dedicated to ship performance in dynamic ice. This can be categorized into two main approaches. The first category takes a data-driven approach. Kubat et al. (2012; 2016) analyzed the correlation between occurrences of ship besetting with ice forecast data, while Montewka et al. (2015) focused on establishing a probabilistic model based on ship and environmental data to predict ship performance in dynamic ice. Similä and Lensu (2018) and Lensu and Goerlandt (2019) used various data to estimate ship speed in varying ice conditions but lack a specific focus on dynamic ice. The second category is based on engineering modelling. Riska et al. (1995) proposed a modelling framework for ships in dynamic ice and proposed ice compression index to account the contact between dynamic ice and midship sections. Kaups (2011) and Külaots et al. (2013) modelled the ship resistance in dynamic ice.

Notwithstanding the significance of existing work, the current approaches still have significant limitations for estimating a ship's operability in dynamic ice. The data-driven approach requires sufficient and high-resolution data in order to obtain an applicable prediction for a specified ship. For example, the investigation by Kubat et al. (2012; 2016) only targeted one ship. Therefore, there is considerable uncertainty about the performance of another vessel even in the same conditions. The probabilistic model by Montewka et al. (2015) has the advantage of making a high-level abstraction of the complex physical processes, but the modelling is also limited to a certain ship type due to limitations of the model training data. The engineering models can predict the performance of any specified ship but have to tackle the complex dynamic ice-ship interaction process. So far, engineering models mainly focused on calculating ship resistance for a ship. The proposed formula based on experiments by Riska et al. (1995) present a plausible method to model ship performance in dynamic ice but has not yet been validated. The resistance calculation scheme for a vessel in compressive ice by Kaups (2011) and Külaots et al. (2013) has the limitation of static status assumptions, i.e. the resistance is calculated only for a steady speed. When the ship speed varies with time during a transit, the calculation scheme may not be applicable. Therefore, a dynamic transit model is needed for estimating a ship's operability in dynamic ice.

In addition, as mentioned earlier, dynamic ice also poses challenges to escort operation. And there is no specific model yet focusing on estimating ship performance for escort operation in dynamic ice. Goerlandt et al. (2017) made a data analysis of ship escort and convoy operations for different ice conditions, but do not focus on the conditions of getting stuck in dynamic ice. Zhang et al. (2018; 2019) proposed models for the vessel dynamics in escort and convoy operations but not considering dynamic ice condition. Therefore, there is a need for including escort operation modelling in dynamic ice condition.

Considering the above, this paper aims to establish a way to assess ship operability in hazardous dynamic ice conditions so that preparatory operability information for a specified ship can be estimated in terms of forecasted environmental conditions. First, this paper proposes transit models for both independent navigation and escort operation in dynamic ice. Then, based on the transit models, an operability index is proposed for assessing ship operability in dynamic ice. This index indicates directly whether the condition is favorable, risky or unfavorable for a specified ship. This index is intended to be used for visualizing the operability of vessels for ship routing purposes, or for maritime emergency response planning in ice conditions such as marine pollution preparedness and response planning. In this work, dynamic ice here is restricted to a level ice field or a very large level ice floe. Finally, case

studies of independent and escort navigation in a realistic dynamic ice conditions are investigated and compared with the simulated results and proposed operability index, as a validation of the proposed method.

The following Section 2 introduces the method proposed in this paper. Section 3 shows details of the case studies as well as corresponding validation and sensitivity analysis results. In Section 4, a discussion is presented, and Section 5 concludes.

## 2. Proposed method

This section is comprised of two parts. The first part focuses on the modelling method of ship transit in dynamic ice for independent navigation and escort operations, respectively. The method starts from independent navigation modelling in dynamic ice, based on the simplified framework (Fig. 1) by Riska et al. (1995). Hence, ship resistance in dynamic ice is decoupled into level ice breaking induced resistance and additional dynamic ice contact resistance, bases on which a dynamic transit model is established. Further, this model for independent navigation is extended to escort operations. The second part describes the proposed ship operability index in dynamic ice based on the developed transit models for independent navigation and escort operations, which enables a quick assessment of a specified ship's operability in relevant ice conditions. The intention of the ship operability index is that it can be used as an information layer in navigational charts for routing purposes, or as an information layer in oil spill response information systems.

### 2.1. Modelling ship transit in dynamic ice

#### 2.1.1. Independent navigation

Independent navigation in dynamic ice means that a ship sails by itself in level ice or a large ice floe which drifts under the influence of wind and current. In the dynamic ice condition, turning of the ship may lead to loss of ship speed and lead to a higher risk of getting stuck. In this paper, ship transit is simplified so that the ship is travelling in a straight course with the maximum power setting. Similar as the transit model in ridged ice (Kuuliala et al., 2017), the equation of motion for a rigid ship is expressed as in Eq. (1).  $M$  is the ship mass,  $a_j$  is acceleration,  $T_{nj}$  is the total net thrust concerning the difference between propeller thrust and open water resistance,  $R_{L,j}$  is total resistance from level ice, and  $R_{A,j}$  is the additional dynamic ice resistance at time step  $j$ .

$$Ma_j = T_{nj} - R_{L,j} - R_{A,j} \quad (1)$$

The acceleration can be calculated when obtaining the ship resistance and net thrust, and is further used to estimate the ship position and velocity by following Newmark's numerical integration method (Newmark, 1959) as in Eqs. (2) and (3). This approach is also adopted by Kuuliala et al. (2017) in the transit modelling for ships in ridged ice.  $v_j$  and  $x_j$  are speed and position at time step  $j$ ;  $dt$  is the length of time step.

$$v_j = v_{j-1} + \frac{1}{2}(a_{j-1} + a_j)dt \quad (2)$$

$$x_j = x_{j-1} + v_{j-1}dt + \left(\frac{1}{3}a_{j-1} + \frac{1}{6}a_j\right)dt^2 \quad (3)$$

The resistance and net thrust are dependent on the location and speed, therefore the acceleration, speed and location of a time step are interdependent. Iterations are conducted with each time step to solve the transit Eqs. (2) and (3). In the current model implementation, minimum ten iterations are set, or fewer if the convergence limit of 1E-3 is achieved between two consequent accelerations in the iterations, as is done in Kuuliala et al. (2017), where a transit model for a ship in ridged ice is created. To solve Eq. (1), the level ice resistance, additional dynamic ice resistance and net thrust are needed. Therefore, the following focuses on calculating those three components.

The resistance encountered by a ship sailing in dynamic ice is divided into resistance from breaking through the level ice sheet and additional

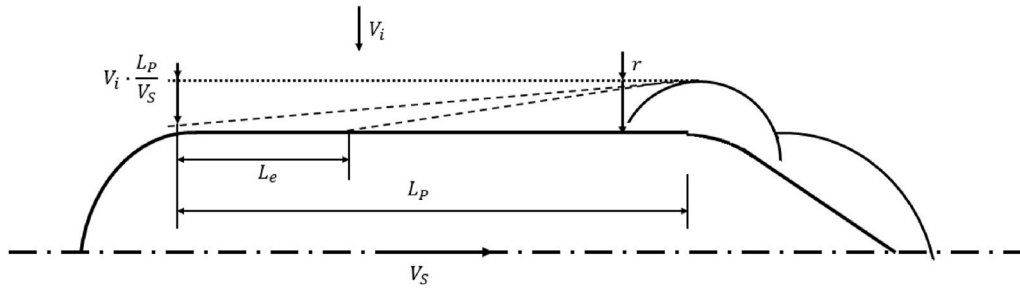


Fig. 1. A ship in dynamic ice, based on Riska et al. (1995).

resistance from ice-ship interaction in the parallel midship section, as shown in Fig. 1. Therefore, the two resistance components need to be modelled separately.

According to Kämäräinen (1993) and Li et al. (2018), the method for level ice by Lindqvist (1989) gives a good estimation of level ice resistance. Therefore, it is applied here for accounting for the level ice resistance. The total level ice resistance  $R_L$  is composed of three parts, namely breaking  $R_B$ , crushing  $R_C$  and submersion  $R_S$ , which are expressed as below:

$$R_L = (R_B + R_C) \left( 1 + \frac{1.4v}{\sqrt{gh_i}} \right) + R_S \left( 1 + \frac{9.4v}{\sqrt{gL}} \right) \quad (4)$$

$$R_B = 0.003\sigma_f B h_i^{3/2} \left( \tan\psi + \mu \frac{\cos\varphi}{\sin\alpha \cos\psi} \right) \left( 1 + \frac{1}{\cos\psi} \right) \quad (5)$$

$$R_C = 0.5\sigma_f h_i^2 \frac{\tan\varphi + \mu \cos\varphi / \cos\psi}{1 - \mu \sin\varphi / \cos\psi} \quad (6)$$

$$R_S = \rho_\Delta g h_i \left( \frac{T(B+T)}{B+2T} + \mu \left( 0.7L - \frac{T}{\tan\varphi} - \frac{B}{4\tan\alpha} + T \cos\varphi \cos\psi \sqrt{\left( \frac{1}{\sin\varphi} \right)^2 + \left( \frac{1}{\tan\alpha} \right)^2} \right) \right) \quad (7)$$

where  $v$  is ship speed;  $L$ ,  $B$ ,  $T$  are ship length, breadth and draught;  $\alpha$ ,  $\varphi$ ,  $\psi$  are ship open water angle, stem angle and flare angle and  $\psi = \arctan(\tan\varphi / \sin\alpha)$ .  $\mu$  is the friction coefficient between ship and ice;  $h_i$  is ice thickness;  $\sigma_f$  is ice flexure strength;  $g$  is gravity acceleration and  $\rho_\Delta$  is the density difference between ice and water. All variables and parameters are in SI units.

The additional resistance caused by the dynamic ice is considered here as additional friction resistance to the ship, caused by the horizontal ice forces onto the midship section. When the ship maintains its movement in ice, the horizontal ice force is dominated by the interaction between the ice and vertical midship hull, where crushing happens. Although bending failure may also occur, it is considered as a more marginal phenomenon (Li et al., 2019). Kujala and Arughadoss (2012) studied crushing pressures from model-scale laboratory and full-scale measurements and suggested following pressure-area relation:

$$p = 0.42A^{-0.52} \quad (8)$$

where  $p$  is the pressure (in MPa) and  $A$  is the contact area, in SI unit.

Therefore, the additional friction resistance to the ship is expressed as

$$R_A = 2\mu p h_i L_e \quad (9)$$

where  $R_A$  is the additional resistance;  $\mu$  is the friction coefficient be-

tween ship and ice;  $p$  represents crushing pressure in equation (8),  $h_i L_e$  together stands for the contact area,  $h_i$  denotes ice thickness and  $L_e$  means effective contact length, all in SI units.

In order to calculate the additional resistance, the problem can then be reformulated to identify the effective contact length between the parallel midship section and dynamic ice. As shown in Fig. 1, it is considered that the cusp broken at the bow shoulder determines the distance between the ice edge and ship. Wang (2001) and Su et al. (2010) applied the following equations to calculate the breaking radius:

$$r = C_l l_c (1 + C_v v) \quad (10)$$

$$l_c = \sqrt[4]{\frac{E h_i^3}{12(1-\nu^2)\rho_w g}} \quad (11)$$

where  $r$  is the breaking radius, i.e. the distance from ice edge to ship as in Fig. 1;  $C_l$  and  $C_v$  is the empirical coefficients;  $v$  is the ship speed.  $l_c$  is the characteristic length;  $E$  is the elastic modulus of ice,  $\nu$  is Poisson's ratio,

$h_i$  is ice thickness,  $\rho_w$  is the density of water and  $g$  is gravity acceleration. They are in SI units.

The effective contact length  $L_e$  is regarded as the contact length between the ice edge and the parallel midship section considering that the ice edge is moving linearly with time, as illustrated in Fig. 1. Therefore, the contact length can be determined in each time step based on the ship speed and ice drift speed so that the additional dynamic ice resistance can be obtained for the motion equation (Eq. (1)) as well.

The solution of the motion equation of the ship also requires the net thrust. The net thrust concerns the difference between propeller thrust and open water resistance, and hence represents the thrust available to overcome additional resistance from ice. According to Riska et al. (1997), the net thrust can be estimated by:

$$T_n = T_b \left( 1 - \frac{1}{3} \frac{v}{v_{ow}} - \frac{2}{3} \left( \frac{v}{v_{ow}} \right)^2 \right) \quad (12)$$

Table 1

Values for bollard pull coefficient  $K_e$ , based on Riska et al. (1997).

Number of propellers	Type of propellers	
	Controllable pitch	Fixed pitch
1	0.78	0.7
2	0.98	0.88
3	1.12	1.01

$$T_b = K_e (P_d D_p)^{2/3} \quad (13)$$

where  $T_n$  is the net thrust,  $v$  is the ship speed,  $v_{ow}$  is designed ship open water speed,  $D_p$  is the propeller diameter, they are in SI units.  $T_b$  is the bollard pull (in kN),  $P_d$  is power (in kW).  $K_e$  is a coefficient accounting propeller characteristics. The values are listed in Table 1.

Based on the above formulations, the transit modelling for independent navigation in dynamic ice is fully specified and the equation of motion (Eq. (1)) can be solved. Each time when the ship updates its location in the modelling procedure, the corresponding ice thickness and drift speed information can be derived from the relevant or preset ice dataset. Furthermore, the corresponding ship speed which will be used in the ship operability index, see details in Section 2.2, can be calculated.

### 2.1.2. Escort

Escort operation means that an icebreaker breaks through the dynamic ice field and that a conventional ship follows the icebreaker at a certain distance (Rosenblad, 2007). The main principle for the numerical transit simulation for this operation is the same as the independent navigation elaborated in Section 2.1.1. However, this situation involves two ships. The leading ship operates the same as in independent navigation. The following ship however may encounter different ice situations under the influence of the leading ship.

The dynamic ice edge is affected by the leading ship, as shown in Fig. 2, and the condition of the ice edge after the leading ship influences the assisted ship. Generally, two situations can be distinguished: S1 and S2 as shown in Fig. 2. S1 is the situation that the assisted ship navigates in channel ice broken by the leading ship and the ice edge reaches the assisted vessel at a position abaft the bow shoulder, or that the ice edge does not reach the ship side. S2 is the situation that the channel broken by the leading ship is closing and has become narrower than the width of assisted ship so that the assisted ship needs to break ice to go forward.

In S1, the total resistance is due to two parts: channel ice resistance and additional resistance from dynamic ice. The estimation of the additional resistance caused by the dynamic ice can be calculated using Eqs. (8) and (9), when the effective contact length is determined for each time step. If there is no effective contact, the additional dynamic resistance is zero. The channel ice resistance estimation uses formulas proposed by Riska et al. (1997), i.e.

$$R_{CH} = \frac{1}{2} H_F^2 C_p \left( \frac{1}{2} + \frac{H_M}{2H_F} \right)^2 \left( B + 2H_F \left( \cos\delta - \frac{1}{\tan\gamma} \right) \right) (\mu \cos\varphi + \sin\psi \sin\alpha) + C_m L_p H_F^2 + \rho_{\Delta} g \left( \frac{LT}{B^2} \right)^3 H_M A_{WF} F_n^2 \quad (14)$$

$$H_F = H_M + \frac{B}{2} \tan\gamma + (\tan\gamma + \tan\delta) \sqrt{\frac{B \left( H_M + \frac{B}{4} \tan\gamma \right)}{\tan\gamma + \tan\delta}} \quad (15)$$

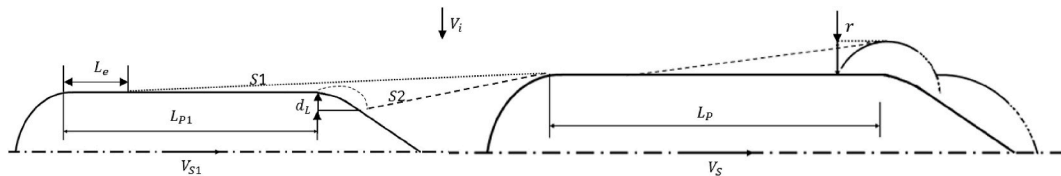


Fig. 2. Escort in dynamic ice.

where  $R_{CH}$  is the channel ice resistance,  $H_M$  is the thickness of brash ice in the middle of the channel,  $H_F$  describes the thickness of the brash ice which is displaced by the bow and moved to the side against the parallel midbody.  $\delta$  and  $\gamma$  are the slope angles of the side wall of brash ice, taken as  $22.6^\circ$  and  $2^\circ$  (Riska et al., 1997).  $C_p$  is a constant that depends on the internal friction angle of the ice rubble and  $C_m$  is a constant dependent on the Possion's ratio and friction coefficient of the ice rubble, taken as  $7500 \text{ kg/m}^2 \text{ s}^2$  and  $45.9 \text{ kg/m}^2 \text{ s}^2$  (Li et al., 2018).  $B$ ,  $L$ ,  $L_p$ ,  $T$  are breadth, length, length of parallel midship section and draught of the ship,  $A_{WF}$  is the waterline area of the foreship,  $\alpha$ ,  $\varphi$ ,  $\psi$  are ship open water angle, stem angle and flare angle.  $\rho_{\Delta}$ ,  $g$ ,  $F_n$  are the different between ice and water, gravity acceleration and Froude number. Except the ones mentioned, the other parameters and variables are in SI units. More details can be found in Riska et al. (1997).

In S2, the assisted ship needs to break some ice which has drifted in front of the ship and meanwhile overcome some channel ice resistance. At the same time, the ice breaking at its bow shoulder also creates a new ice edge which may act on its parallel midship section as in the independent navigation. Therefore, the total resistance is also composed of two parts: the level-channel ice resistance and additional resistance from dynamic ice. There is no formula to calculate this level-channel ice resistance situation yet. Therefore, this situation is considered as a combination of channel ice and level ice, calculated by combining the two resistances based on their proportions in front of the ship:

$$R_{LC} = R_L \frac{2d_L}{B} + R_{CH} \left( 1 - \frac{2d_L}{B} \right) \quad (16)$$

where  $R_{LC}$  is the level-channel ice resistance for S2,  $R_{CH}$  and  $R_L$  are channel ice resistance (Eq. (14)) and level ice resistance (Eq. (4)) respectively.  $d_L$  is the distance the ice edge crosses from the ship sideline to the center line of the ship, see in Fig. 2.  $B$  is ship breadth. They are in SI unit. If the channel is totally closed, it is equivalent to the situation that the ship is navigating in level ice.

The calculation of additional resistance from dynamic ice for assisted ship in S2 follows the same principle as independent navigation described in Section 2.1.1 and applies equations (5)–(8). The resistances for assisted ship in escort operation can be calculated as mentioned above. In addition, the modelling of the net thrust and the motion equation for escort operation remains the same as in the independent navigation situation elaborated in Section 2.1.1.

## 2.2. Ship operability index in dynamic ice

The ship transit modelling in dynamic ice enables an estimation of ship performance under given conditions. However, in order to present the information concerning the risk of getting beset in dynamic sea ice, an easier manner, comprehensive but simplified information of the

ship's navigational capability is required for various conditions. For example, if information about the limiting ice conditions, including ice thickness and ice drift speed, is known for an independently navigating oil spill response vessel, the decision whether to commence the ship's mission through that ice environment can be made based on the forecasted environment and ice conditions. If the vessel cannot safely operate independently, information about whether having the vessel assisted by an icebreaker in the prevailing ice conditions can be useful. Similarly, potentially hazardous areas can be avoided in route planning or in a routing algorithm. Therefore, this section focuses on developing this comprehensive and practically useful information for both independent and escort navigations. This is achieved by defining and operationalizing a ship operability index which is composed of two parts: a base index defining a basic operational category, i.e. favorable, risky or unfavorable and a degree index reflecting the operational degree of severity within each category. More details are given in the following section.

### 2.2.1. Ship operability index for independent navigation

For ships navigating independently, the relevant variables are ship-related parameters and environmental related conditions. The ship-related parameters are relatively constant if a ship and its navigation status are decided, thus the ship operability estimation is primarily based on environmental conditions, specifically ice thickness and ice drift speed. In general, the operability can be categorized as favorable, risky and unfavorable. Here, favorable is defined so that ship speed at the end of a defined simulation period is over 2 kn. Risky is defined here as the condition that the ship speed drops to the interval between 0 and 2 kn, whereas unfavorable means that the ship is stopped by the ice, i.e. that it gets stuck in the dynamic ice. A base operability index is allocated to each operability category, i.e.

$$OP_b = \begin{cases} 0, & v \geq 2 \\ 1, & 0 < v < 2 \\ 2, & v = 0 \end{cases} \quad (17)$$

where  $OP_b$  is base operability index and  $v$  is ship speed in kn.

The base operability index makes it possible to digitize the three operability categories. However, it lacks the ability to show the degree of operability within each category for a more accurate representation of the operability, e.g. reflecting the difference between 1.1 and 1.9 in risky category. Therefore, a degree index is introduced to show how severe it is inside each category based on the degree of speed drop:

$$OP_d = \frac{K_v - K_{v_{min}}}{K_{v_{max}} - K_{v_{min}}} \quad (18)$$

where  $OP_d$  is the degree index,  $K_v$  is the speed drop rate based on the initial and final speed for the defined simulation period  $t$ ,  $K_v = (v_t - v_0) / t$ .  $K_{v_{min}}$  and  $K_{v_{max}}$  are the minimum and maximum speed drop rate in corresponding category.  $OP_d$  is in the range of 0–1.

$OP_b$  determines the basic category based on the final ship speed and  $OP_d$  reflects the severity degree within each category. By adding degree index  $OP_d$  to the base index  $OP_b$ , the defined ship operability index  $OP$  is formulated as expressed in formula (19). More specifically,  $OP_b$  can be regarded as the integer part of  $OP$  and  $OP_d$  can be regarded as decimal part of  $OP$ .

$$OP = OP_b + OP_d = \begin{cases} 0 \sim 1, & \text{Favorable} \\ 1 \sim 2, & \text{Risky} \\ 2 \sim 3, & \text{Unfavorable} \end{cases} \quad (19)$$

The  $OP$  index is derived based on the ship speed at the end of the transit simulation in dynamic ice. Here, the simulation time is set as 10 min, i.e. it is considered that the dynamic ice the ship sails in within 10 min is always complete level ice condition, which is a quite strict condition because in practice, the ice condition varies a lot. There will not be always level ice, and the ice will be fractured or deformed when a

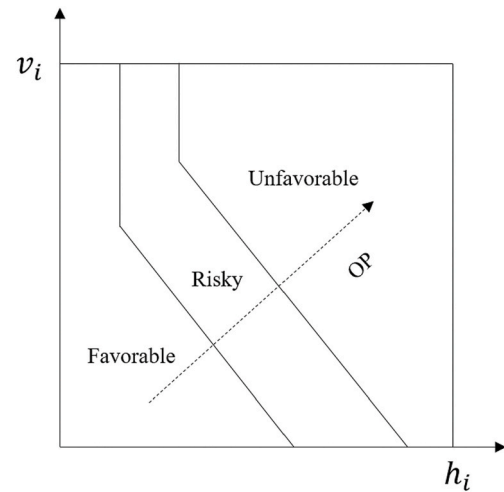


Fig. 3. A schematic diagram: Ship operability index  $OP$  over various ice conditions  $(h_i, v_i)$ .

ship is sailing inside.

One  $OP$  index can be obtained for each pair of ice thickness and ice drift speed  $(h_i, v_i)$ , where  $h_i$  influences both level ice resistance and additional added resistance from dynamic ice through its effect in both resistance equations and  $v_i$  influences the additional added resistance component through its effect in the effective contact length between the parallel midship section and dynamic ice in each time step. Thus, the overall matrix of  $OP$  index for a ship can be derived by simulating various combinations of  $(h_i, v_i)$ . The overall operability for a certain ship in various ice conditions can then be presented as in Fig. 3. Fig. 3 as represented in this section is only a schematic diagram, not reflecting realistic information for  $OP$  map in terms of  $(h_i, v_i)$ . When the practical ice condition is known, a quick assessment of the ship's operability in that condition can be made based on a real obtained operability map like Fig. 3.

### 2.2.2. Ship operability index for escort operations

Escort is different from independent navigation because it relates to not only the ice condition, but also the operations between the two ships. Therefore, in addition to the ice thickness and drift speed, the operability is affected by the escort distance between the two ships and the escort speed. Based on practical understandings and information from the literature (Zhang et al., 2017, 2018, 2019), it is assumed that the escort operation follows a principle, i.e. the leading ship and assisted ship try to maintain a steady escort distance and a steady escort speed. If the leading ship and assisted ship cannot maintain the preset escort speed in a certain ice condition, the assisted ship's real speed will be followed as the escort speed. Detailed implementation features of the proposed algorithm include:

- 1) the leading ship closely follows the assisted ship's speed;
- 2) when the assisted ship's speed is less than two knots, the leading ship increases its speed to avoid getting itself stuck;
- 3) when the leading ship cannot maintain its speed, the assisted ship will try to slow down as well to avoid collision;
- 4) when the assisted ship cannot fully stop and reaches the leading ship, it is considered as a potential collision, which is categorized as unfavorable condition.

Based on these, the operability of the ships can be simulated over a set of ice condition and operation condition,  $(h_i, v_i, D, v_{escort})$  following the same procedure in Section 2.2.1. A similar mapping as in Fig. 3 for both ships can be obtained, however over the four variables  $(h_i, v_i, D, v_{escort})$ . The operability of the assisted ship is in particular focus to assess

the operability of the escort operation.

### 3. Method validation: case studies comparing the proposed method with observations

This section focuses on case studies of independent navigation and escort operation in real dynamic ice, providing a validation of the capability of the ships in real dynamic ice conditions with the ship operability as simulated by the method described in Section 2.

Empirical cases of a ship which has gotten stuck in dynamic ice are valuable information sources to study the ship operability. Due to the complexity of real situations, there are various reasons for a ship to stop. Therefore, the only plausible way to confirm a ship getting stuck in a dynamic ice field is to rely on observations in the corresponding context. The cases here are determined based on the SAFEWIN project cruise report (Vedenpää, 2011). It describes events where the research vessel got stuck in severe dynamic ice scenarios and reported other nearby vessels becoming beset in ice. According to the reported time and location, the scene is recreated using data from the Automatic Identification System (AIS) in this region for the reported vessel and other nearby vessels as well as relevant ice information. Three ships are selected, which represent validation scenarios for the proposed model for operability of independent navigation and escort in dynamic ice conditions.

Reconstructing case studies of ships in the dynamic ice requires different detailed information and data sources as the process of a vessel becoming stuck in ice occurs over a relatively short time period, as found also e.g. in Montewka et al. (2015). Hence, the resolution of key data sources should be sufficiently high, especially the ship speed. The general data related to the case study scenarios are described in Section 3.1, whereas the validation results and sensitivity analysis are shown in Section 3.2.

#### 3.1. Data and information sources

The case study scenarios concern two operation modes and three ships as shown in Table 2. In independent navigation, the ice-breaking research vessel Aranda became beset in ice at around 22:00. Another icebreaker Nordica is selected for comparison with Aranda in the same period. In escort operation, Nordica is the leading ship, while Envik is the assisted vessel. The relevant data and information consist of three parts: ship data, environmental data, and operational data. In the following sections, these are described in turn.

##### 3.1.1. Ship data

Ship data refers to the ship related parameters required for estimating the vessel performance according to Section 2.1.1 and 2.1.2, such as vessel dimensions, power, etc. Aranda is a Finnish research vessel with ice breaking capability; Nordica is a Finnish icebreaker designed for assisting merchant vessels in winter operations in the Northern Baltic Sea; Envik is a merchant vessel with ice navigation capability. Their main parameters are listed in Table 3.

##### 3.1.2. Environmental data

Environmental data represents the external conditions in which the ship navigates. For the current purposes, this primarily includes the ice condition data, as well as wind data to provide more detailed contextual information. Hindcast data obtained using the HELMI ice model

**Table 2**  
Case study scenarios, based on Vedenpää (2011) and AIS data identification.

Scenario	Operation	Time	Ship
1	Independent navigation	2011-2-24 21:54:27	Aranda
2	Independent navigation	2011-2-24 21:54:27	Nordica
3	Escort	2011-2-24 18:59:26	Nordica - Envik

**Table 3**

Ship parameters of the three vessels in the validation case studies, based on Vedenpää (2011)

Type	Aranda	Nordica	Envik
	Research	Icebreaker	Cement Carrier
Ice class	1A S	PC 3	1A S
Displacement (ton)	1858	12800	5583
Length (m)	59.2	116	96
Breadth (m)	13.8	26	16.5
Draught (m)	5	7	5.2
Open water speed (kn)	13.5	16	12
Power (kW)	3000	15000	2740
Propeller diameter (m)	2.6	4.2	3.05

Note: Ice class classification system: Aranda and Envik (Finnish-Swedish ice class); Nordica (IACS Polar class).

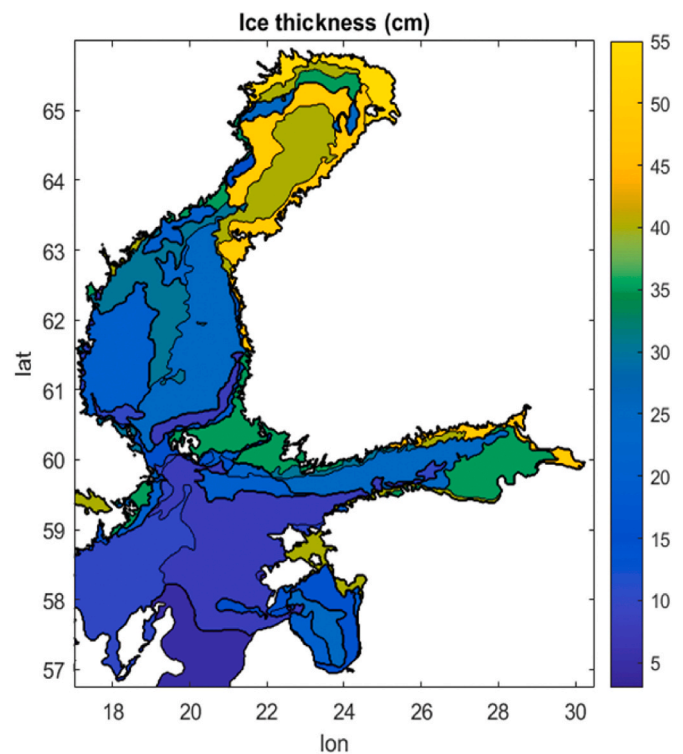


**Fig. 4.** Ice thickness from HELMI model data on February 24, 2012.

(Haapala et al., 2005; Mårtensson et al., 2012) are used as a basis for describing the sea ice conditions, similarly as in Montewka et al. (2015) and Goerlandt et al. (2017). The ice model is discretized in a curvilinear coordinate c-grid and the grid has 415 nodes from west to east and 556 nodes from south to north. It covers an area from coordinates (56.74°N, 16.72°E) to coordinates (65.99°N, 30.48°E) with an increment of 1/30° eastwards and 1/60° northwards, i.e. approximately 1 NM in both directions at 60°N (Goerlandt et al., 2017). The HELMI forecasting model takes thermodynamic and dynamic forcing from the weather prediction model HIRLAM and has been validated against observed ice situations, with good agreement (Lehtiranta et al., 2012). The data concerning ice thickness, ice type and ice concentration are used for ice information here. The general ice thickness map is shown in Fig. 4. The ice type in the region where the three ships operated is level ice according to HELMI data. The ice thickness is extracted based on the routes of the ships, as identified using data from the Automatic Identification System.

In addition, the ice drift condition is vital as one main external factor. The ice drift speed recorded from time to time in the research cruise (Vedenpää, 2011) is used as the local ice drift speed matters most. However, it only reflects the situation at each recorded time, and hence

is not available in a continuous way as is required for the calculation procedures. According to Uotila (2001), ice drift speed is correlated with wind forcing. Therefore, in order to have a better understanding of the ice drift speed, the wind data is used as reference. The wind data is in 10-min interval, derived from a nearest observation station Maalahti Strömmingsbådan (62.98°N, 20.74°E).

### 3.1.3. Operational data

Operational data means the data related to the ships' navigation. Here it mainly concerns ship speed for independent navigation, but also includes the distance between the two ships in escort operation. The historical navigational data record from ships is not available. Therefore, AIS data is used alternatively for deriving the operational data.

AIS is an information exchange platform between vessels and shore organizations and contains static and dynamic data. The dynamic data gives time-dependent data about the location, speed, course and navigational status of vessels, etc. (Goerlandt et al., 2017). As mentioned in the beginning of Section 3, the scenes are recreated by using the AIS data in this region to confirm the reported ships' stuck. Then a detail investigation of the shorter period when ships got stuck is conducted. In this investigation, the resolution of the data is highly important. AIS data is recorded with a varying interval from seconds to minutes, depending on the speed of the vessel and operational status. Therefore, this sets the limit of the AIS data. The data interval for the scenarios in this paper are roughly in 10 s intervals, which is close to best resolution in AIS and considered sufficient for a detailed investigation of ship operations.

In escort operations, the distance between the icebreaker and the assisted vessel is also important information. The distance is calculated based on the coordinates data of the two ships, which are interpolated for the same timestamp first. In addition, the calculated distance is the distance of the locations of the AIS transponders. In order to obtain the real distance between the two ships, the location of AIS transponders are assumed in the bridge area. The distance to ship bow for assisted ship and the distance to ship stern for leading ship are deduced from the calculated distance from coordinates, as in Goerlandt et al. (2017). Furthermore, the simulation considers only 2D waterline condition, thus the distance in the simulation requires the calculated real distance to add stern length of the leading ship and bow length of the assisted ship.

## 3.2. Case study results and sensitivity analysis

### 3.2.1. Case study results: comparing the proposed method with observations

The method in Section 2 is applied to the three ships involved in the case studies in Table 2. The same initial ship speed as in the real scenarios is set for the simulation of each ship. For the independent navigation, the ship operability of Aranda (Scenario 1) simulated according to method described in Section 2.1.1 and 2.2.1 is shown in Fig. 5 (left) over serials of  $(h_i, v_i)$  conditions. The observed scenario of Aranda

becoming beset is indicated by a rectangle as well in Fig. 5 (left). The reported ice drift speed is around 0.3–0.4 kn (Vedenpää, 2011), and the ice thickness is 25 cm, as shown by the rectangle in Fig. 5 (left).

It is seen that the rectangle in Fig. 5 (left) extends from the boundary of favorable to the boundary of unfavorable, with the largest part situated in the risky operability category. Therefore, the simulated operability estimation corresponds well with the observed ship operability in this case. Fig. 5 (right) shows the speed drop when Aranda begins to get stuck. Because the recorded ice drift speed is in the range of 0.3–0.4 kn, the limit values 0.3 and 0.4 are used in the simulation to compare with the observed AIS data. The simulation using 0.4 kn ice drift speed is quite close to the trend from AIS, especially in the end period. The change of the speed in the middle period from AIS data may reflect slight variation of the ice condition. The simulation using 0.3 kn ice drift speed indicates that Aranda is still able to navigate if ice drifts at this speed. When tracking back to wind records, it is found that wind speed reaches the maximum of 15.6 m/s at 22:00, i.e. the time at which Aranda became stuck in ice. It is the daily maximum wind speed and is 1 m/s higher than the speed at 21:50. Therefore, the ice drift speed is more likely to be close to 0.4 kn, thus causing Aranda to become stuck. It also explains why Aranda can still sail before 22:00. Therefore, ship operability of Aranda is overall well estimated by the proposed method.

Another simulation for icebreaker Nordica is conducted as it is also in this region, while no reports were made of its getting beset in ice. Therefore, the operability simulation of this vessel can contribute to establish validity of the proposed method for a different ship. The same ice condition as for Aranda is applied to Nordica and its operational status, i.e. its initial speed is derived to reconstruct the ship condition at the same time when Aranda gets stuck. Fig. 6 (left) shows that in general, Nordica operates in favorable ice conditions for its ice-going capability, so that there are no issues with its operability in the prevalent compressive ice conditions. Fig. 6 (right) demonstrates the speed trends from simulations and the AIS records. It is seen that the observed ship speed from AIS matches the simulation of the two different ice drift speeds relatively well.

From the above presented case studies for independent navigation, the comparison suggests that the method can adequately estimate the ship operability on a general level and the changes of the ship speed on a detailed level. The method furthermore appears to be adequately sensitive to the ice-going capability of different ships.

In the selected escort operation, the simulation escort distance at the time for Envik getting stuck is calculated as 430 m following steps described in Section 3.1.3. The speed of Envik is also derived from AIS data as escort speed. The operability of the assisted vessel is of concern in escort operation. In Fig. 7, the ship operability index of Envik is plotted over serials of  $(h_i, v_i)$  conditions, which is shown together with the observation of the reported case of the vessel becoming stuck in ice. As there is no direct ice drift speed reported in that time period, the ice

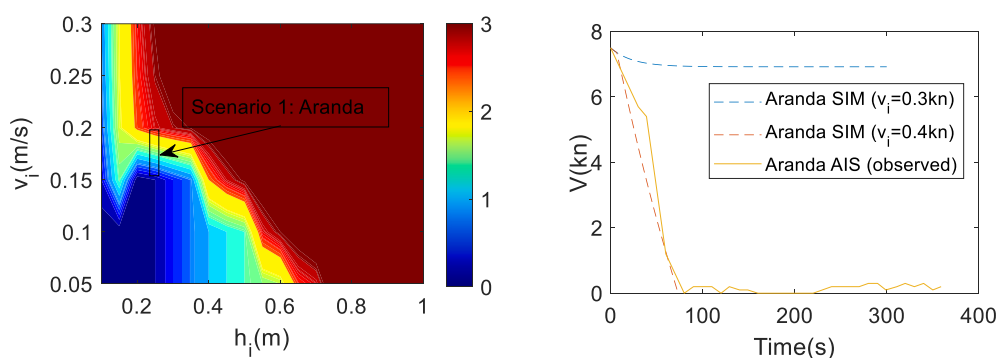


Fig. 5. Scenario 1: Aranda ship operability (left) and speed drop (right) comparison. Scale 0–1 represents favorable, 1–2 represents risky and 2–3 represents unfavorable.

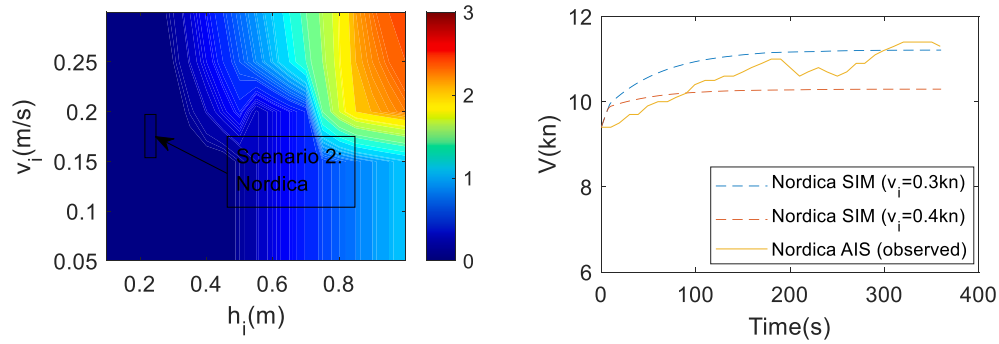


Fig. 6. Scenario 2: Nordica ship operability (left) and speed (right) comparison. Scale 0–1 represents favorable, 1–2 represents risky and 2–3 represents unfavorable.

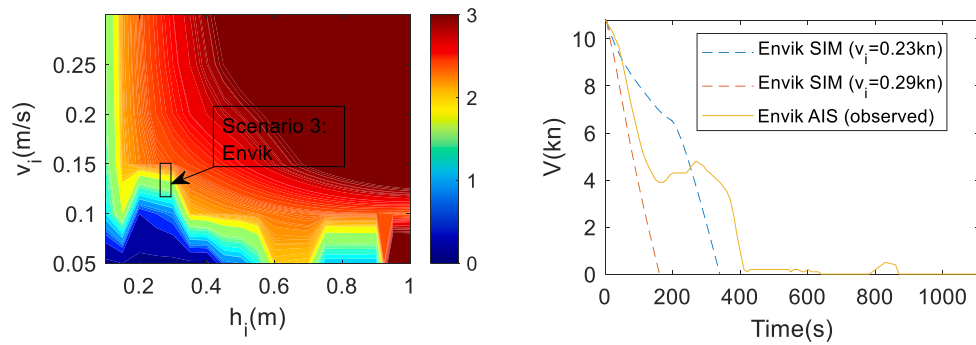


Fig. 7. Scenario 3: Envik ship operability (left) and speed (right) comparison. Scale 0–1 represents favorable, 1–2 represents risky and 2–3 represents unfavorable.

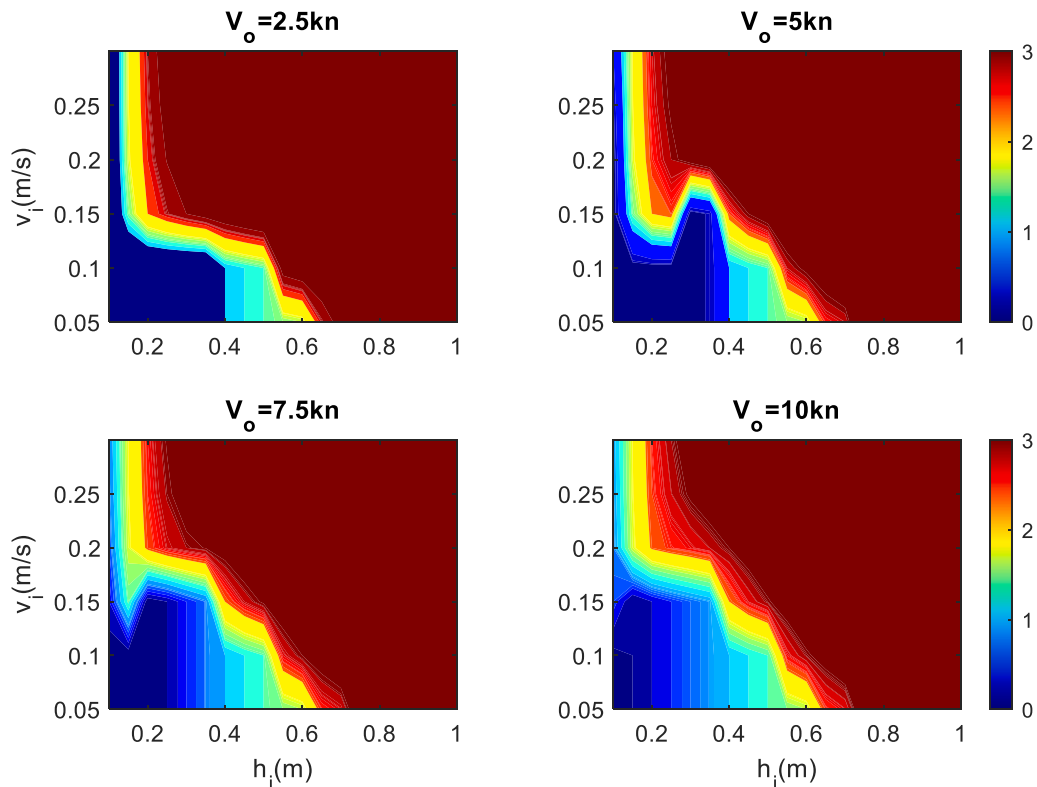


Fig. 8. Aranda ship operability over different initial ship speeds. Scale 0–1 represents favorable, 1–2 represents risky and 2–3 represents unfavorable.

speed is estimated based on the wind speed. Based on Uotila (2001) and Montewka et al. (2015), it is assumed that the ice speed is linearly affected by the wind. Hence, the ratio of the wind speed reported for scenario 3 and scenario 1 is used as a factor to multiply the ice speed in Aranda case. This results in an ice drift speed of 0.23–0.29 kn during this period. This ice drift speed range is shown by the rectangle in Fig. 7 (left) and it covers the risky and unfavorable parts in the simulated operability map in Fig. 7 (left). It should be noted that the interval of both ice thickness  $h_i$  and ice drift speed  $v_i$  for the ship operability index simulation is 0.05, therefore the operability index result between e.g. 0.1 m/s and 0.15 m/s ice drift speed at 0.25 m ice thickness is interpolated. If the boundary condition of ice drift speed, 0.23 kn and 0.29 kn is used, the operability result is unfavorable as can be judged from simulated speeds in Fig. 7 (right). This difference is remained here instead of improving the resolution of intervals of parameters for Fig. 7 (left) is to highlight the importance of selection of the interval when conducting the ship operability index simulation and mapping. Fig. 7 (right) shows the speed drop of both simulations and observed AIS data. The speed trend from the observed case is generally situated between the two bounding simulation scenarios based on the estimated ice speed. However, it is apparent that Envik encountered some varying ice conditions, e.g. some ice floes with open water involved among them, in this scenario as it managed to keep the speed at around 4 kn for a period of time before getting stuck. Nevertheless, its speed continued to drop at a similar rate soon and it got stuck. This varying ice condition cannot be reflected in the simulation result as the simulation considers the ship encounters level ice continuously in the simulation period.

### 3.2.2. Sensitivity analysis: effects of operational variables on ship operability index

Sensitivity analysis is used to ascertain how a given model output depends upon the input parameters and check the robustness and reliability of its analysis, which contributes to the validation of a proposed model (Saltelli et al., 2009). The operability assessment of the three ships in various environmental conditions is shown in the operability

maps in Figs. 5–7, as an initial validation of the proposed method. These results are based on the operational conditions derived from observed case studies. The effects of the operational variables, i.e. ship initial speed  $v_o$  for independent navigation and escort distance and speed ( $D$ ,  $v_{escort}$ ) for escort operation, on the ship operability in dynamic ice are not studied yet. Therefore, this section focuses on the sensitivity analysis of operational variables in the proposed method, as a further validation.

In independent navigation, the main operational variable is initial speed. Fig. 8 shows the ship operability index map of Aranda for different initial ship speeds (2.5, 5, 7.5, 10) kn. In general, a higher initial speed does not extend the ship operability to higher maximum ice thicknesses, but it does extend the operability to higher ice drift speeds. This can be explained by considering that a higher ship speed will enable the ship to avoid contact between its parallel midship and the dynamic ice on the sides. In addition, a trend can be observed in Fig. 8 that although the favorable area increases with higher ship speeds, there is a more outspoken speed loss, i.e. the color is more diverse for favorable category. This is consistent with the fact that a higher initial speed leads to a proportionally larger speed loss compared to lower initial speeds. Another point is that the change in operability is not always linear. For example, when the initial ship speed is 5 kn, the operability at 0.3 m ice thickness is better than at 0.2 m. This can be explained that the ice cusp radius induced by that ship speed and ice thickness is more favorable for the ship to escape the contact from the dynamic ice.

Fig. 9 shows a similar sensitivity analysis for the effects of the initial ship speed for Nordica. The observed effects are relatively smaller than for the Aranda cases shown in Fig. 8. Therefore, the initial ship speed has a limited effect on ship operability for more powerful icebreakers. This can be explained by the fact that powerful icebreakers can already handle more severe ice conditions even at relatively low ship speeds with adequate power.

For escort operations, the operational variables include the escort distance and escort speed. The escort distance and speed are taken here as the initial distance between the vessels and initial speed of the assisted ship. As described in Section 2.2.2, the ships will try to maintain

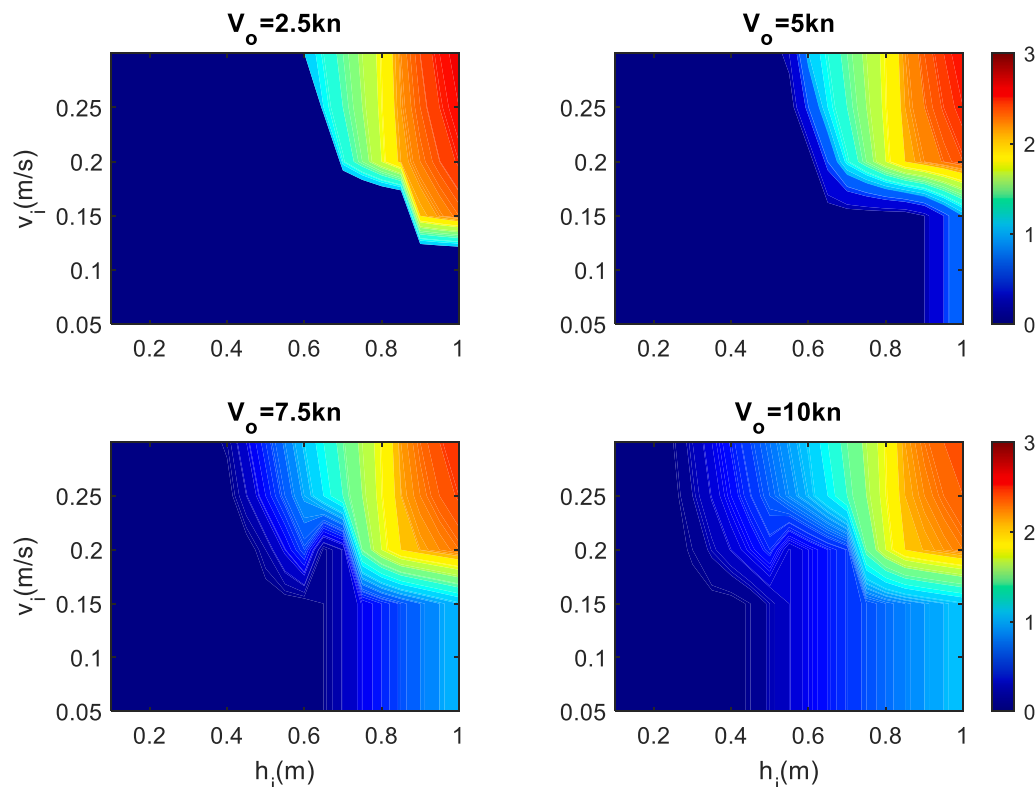
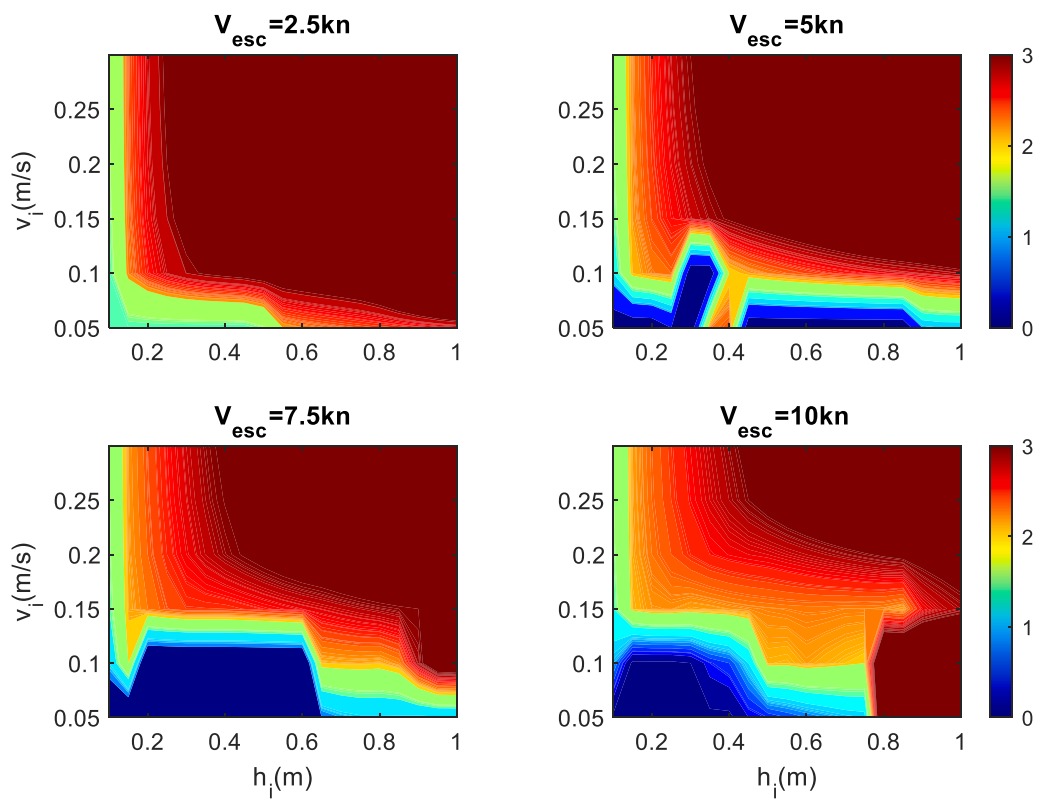
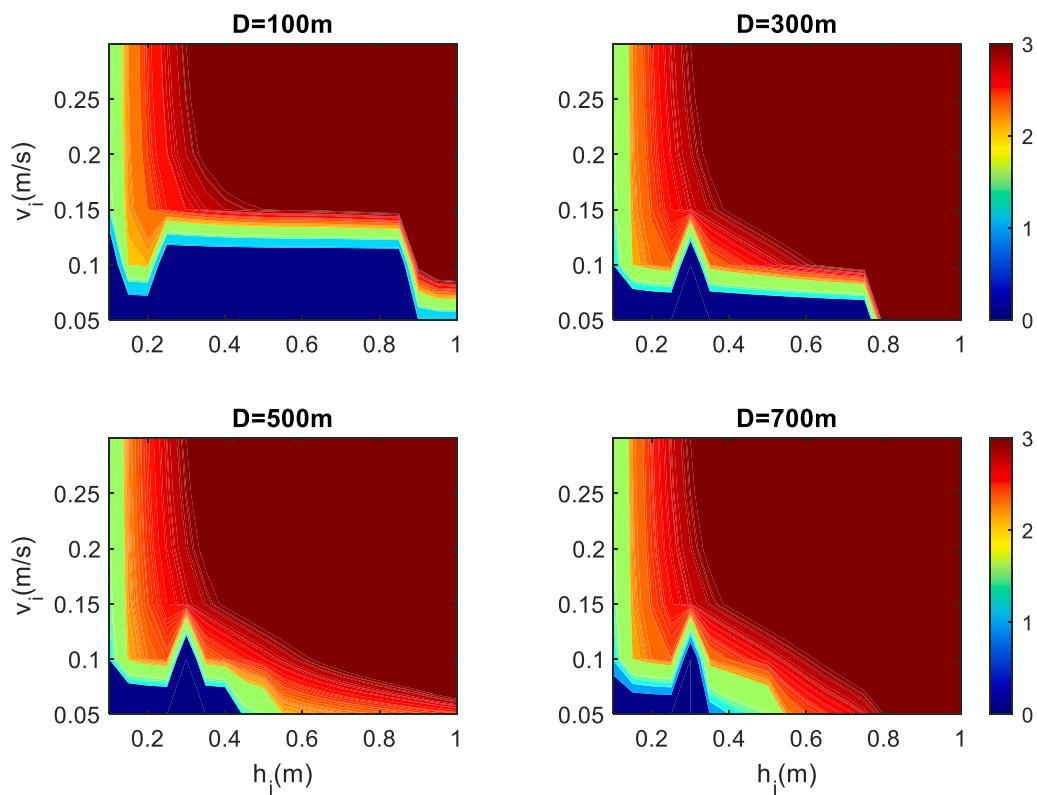


Fig. 9. Nordica ship operability over different initial ship speed. Scale 0–1 represents favorable, 1–2 represents risky and 2–3 represents unfavorable.



**Fig. 10.** Nordica-Envik escort: Envik ship operability over different escort ship speed when  $D = 200m$ . Scale 0–1 represents favorable, 1–2 represents risky and 2–3 represents unfavorable.



**Fig. 11.** Nordica-Envik escort: Envik ship operability over different escort distance when  $v_{escort} = 5kn$ . Scale 0–1 represents favorable, 1–2 represents risky and 2–3 represents unfavorable.

both distance and speed during escort. The principles in Section 2.2.2 are followed if the ships are not able to continue in the initial states. Fig. 10 shows the sensitivity analysis results for the effects of the escort speed when the escort distance is 200 m. A low escort speed (2.5 kn) mostly leads to risky and unfavorable operability. With increasing escort speeds, e.g. 5 kn, the region of favorable ship operability of Envik extends to a large ice thickness domain by following Nordica. However, the limiting ice drift speed is quite low, i.e. Envik can still relatively easily get stuck in windy conditions. At an ice thickness of around 0.35m, there is an unfavorable condition. This seems an unfavorable ratio between the ship speed and ice cusp radius induced by that ship speed and ice thickness where the assisted ship is caught by the ice edge created by the leading ship. With a further increased escort speed (7.5 kn), the ship operability extends also to wider ice drift speed limits. When the escort speed is high (10 kn), the favorable operation condition vanishes in the large ice thickness region (0.8–1.0 m). This unfavorable operability is caused by the identified potential collision in the simulation as defined in Section 2.2.2. In reality, collision is harder to simulate as there are many factors involved, including human actions (Zhang et al., 2017, 2019). However, it is not focus of this paper. Here, the result can be taken to indicate that very thick ice can cause a large speed drop of the leading icebreaker, which is equivalent to the situation that the leading ship suddenly stops as described by Zhang et al. (2018). Hence, a too high escort speed can more easily lead to a collision and is not a favorable choice under such ice conditions.

Fig. 11 shows the results of the sensitivity analysis for the effects of escort distance on the ship operability. When the escort distance is relatively small (100 m), the favorable operability category for Envik is quite wide in ice thickness direction. This means that thick ice does not represent a significant problem as Envik can follow Nordica quite well when Nordica breaks the way ahead. When escort distance increases, the favorable operability region decreases because the ice starts to drift into the channel after the leading ship, before the assisted ship, which causes operability problems for the assisted ship. Overall, both sensitivity analysis on escort speed and distance shown in Figs. 10–11 indicate reasonable trends as in practice in the escort operation.

## 4. Discussion

### 4.1. Ship transit modelling

Although the case studies in Section 3.2.1 show a reasonable agreement between simulation and real cases from both general operability viewpoint and from the more detailed viewpoint of the speed profile, it is noted that the proposed model has several simplifying assumptions.

First, this paper conducts ship transit modelling for independent navigation extending the modelling framework by Riska et al. (1995) by modelling and integrating each resistance component and thrust in the process. In the estimation of the additional resistance caused by the dynamic ice, it is assumed that the additional nominal pressure follows the pressure-area relationship of Eq. (8) as the result of crushing. However, it is known that not only crushing occurs when the dynamic ice reaches the ship side, but that bending failure may also occur (Li et al., 2019). The difference may be expected to be small as bending does not frequently happen. In addition, without considering the bending phenomenon, the method gives a relatively conservative results, which allows a safety margin when it is practically used. It can be investigated in future work to what extent the bending phenomenon is important in this process as there are few researches on this.

Second, the effective ice edge is considered as the edge determined by the cusp radius as in Eq. (10) and (11), and the effective contact length is detected based on those formulations. There are usually small sharp ice edges between cusps, see e.g. Su et al. (2010), and individual sharp ice pieces can also cause some crushing forces on the ship side before the defined effective ice edge reaches the ship. This may lead the

additional resistance by the dynamic ice to occur earlier than when one only considers effective ice contact length.

Third, cracks are also not considered in the simulation. When the ship creates cracks in the surrounding ice field, the ice may be more broken than in conditions where only cusps caused by bending failure are considered, which leads to less resistance. Finally, the simulation model assumes that the dynamic ice edge moves perpendicular to the ship side linearly with time, while the ice movement in realistic conditions may be in oblique direction and much more complicated.

Based on the validation cases and sensitivity analysis of Section 3, it is found that the model gives reasonable estimates. This suggests that the several above identified simplifying assumptions made in the proposed method compensate one another, although the actual complexity of the ice conditions in the dynamic ice are not accurately accounted for.

The model is further extended to escort operation, which is a more complex operation as it involves two ships. The ice edge affected by the leading ship will further influence the assisted ship. The resistance for a ship breaking through in partial level ice and partial channel ice is simplified by combining a weighted sum of both. The resistance for a ship in this mode needs more research as currently there is no study on this situation. The ice breaking in partial level ice is still considered the same as in level ice, including the formation of cusps. In addition, escort includes cooperation between two ships. The principles in Section 2.2.2 are practically reasonable. However, it should be noted that the assumption that the leading ship will increase its speed to avoid getting itself stuck in ice when the assisted ship's speed is less than two knots may cause some overestimate. Because the leading ship may still be able to keep the low speed in light ice conditions. However, the chance for the assisted ship to not able to maintain its speed is also relatively rare in that light ice conditions. Therefore, the influence for this overestimation can be considered minor. In addition to this, the escort process involves communication and control of powering when ships cannot simply follow the escort speed. The way to accelerate and decelerate ships influences the ship behavior and operability.

### 4.2. Validity of the ship operability method

The new proposed method to assess the ship operability for independent navigation and escort appears to provide reasonable results based on the validation case studies and the presented sensitivity analyses. However, it is advisable to further validate the model in follow-up research, e.g. by investigating more cases through comparing the simulation results with observations. Good case studies require a combination of various sources of high-resolution data so that the scene can be accurately reconstructed. AIS data can provide the operational data for a forensic case study if there is no access to onboard records of operational ship data. However, AIS data has limitations related to the varying time intervals of data reporting. The environmental conditions, AIS antenna setup, and other factors can restrict and affect the reception rate (Last et al., 2015), therefore in many conditions the time interval is in minutes and this kind of time interval is less appropriate for obtaining validation case study. This makes post-case study a bit more difficult. In addition, it is also not enough to only have environmental data derived from models. Real onboard measurement and records for the environmental conditions are vital for further validation studies.

All these factors imply that identifying and defining validation cases studies is a rather cumbersome process, which is one of the reasons why also in this paper there are relatively few validation cases. The limited attention to and difficulties of validating models for ship performance in ice, even for comparatively easier ice conditions such as continuous operation in level ice, has been highlighted as well in the work by Li et al. (2018).

In term of the model application, it has already shown good behavior as seen in the sensitivity analysis. Therefore, it can be a useful tool to generate the operability index map for a ship so that the ship route or oil spill response missions can be planned and fulfilled more successfully.

However, it should be noted that there are still uncertainties which need to be kept in mind in real application. First, there may be still model behavior uncertainties unexposed due to the simplifications and limited validation cases. Second, the uncertainties may also come from the quantification of the environmental conditions, there are still limitations to have the real accurate forecast of the environmental variables to give good inputs to the model. Real ice fields may be comprised of several ice types, such as ridged and rafted ice. Hence, further developing the proposed method to account for combinations of dynamic ice with ridged and rafted ice can be a fruitful avenue for future work as well.

## 5. Conclusions

This paper presents a method to assess the performance of ships in dynamic ice for both independent navigation and escort in dynamic ice. In addition, a ship operability index is suggested, which can be a practically useful tool for ship routing to avoid ship stuck in dynamic ice. Ship operability index can be used as an overall estimation to visualize the operability of vessels based on ice forecast in different sea areas, which is especially useful as an information source for emergency response planning such as marine pollution preparedness and response planning. Case studies show reasonable agreement between the simulated model results and empirical observations reconstructed from available data sources. This, together with plausible model behaviors as tested in a series of sensitivity analyses, suggests a reasonable model validity. Nevertheless, it is advised to further validate the model with other vessel types and in other ice conditions, using various data and information sources.

## CRedit authorship contribution statement

**Liangliang Lu:** Conceptualization, Methodology, Software, Formal analysis, Investigation, Data curation, Validation, Writing – original draft, Writing – review & editing. **Pentti Kujala:** Conceptualization, Writing – review & editing, Supervision. **Floris Goerlandt:** Methodology, Writing – review & editing.

## Declaration of competing interest

The authors declare that they have no known competing financial interests or personal relationships that could have appeared to influence the work reported in this paper.

## Acknowledgements

The work received funding from SIMREC project (CBC 2014–2020), funded by the European Union, the Russian Federation and the Republic of Finland. The work also received funding from the Lloyd's Register Foundation, a charitable foundation, helping to protect life and property by supporting engineering-related education, public engagement and the application of research [www.lrfoundation.org.uk](http://www.lrfoundation.org.uk). The contributions by the third author were undertaken in context of the project 'Safe Navigation and Environmental Protection', thanks in part to funding from the Canada First Research Excellence Fund, through the Ocean Frontier Institute. The authors also thank Fang Li and Mikko Suominen for their valuable comments to the paper.

## References

Beveridge, L., Fournier, M., Lasserre, F., Huang, L., Têtu, P.L., 2016. Interest of Asian shipping companies in navigating the Arctic. *Polar Science* 10 (3), 404–414. <https://doi.org/10.1016/j.polar.2016.04.004>.

Choi, M., Chung, H., Yamaguchi, H., Nagakawa, K., 2015. Arctic sea route path planning based on an uncertain ice prediction model. *Cold Reg. Sci. Technol.* 109, 61–69. <https://doi.org/10.1016/j.coldregions.2014.10.001>.

Goerlandt, F., Montewka, J., Zhang, W., Kujala, P., 2017. An analysis of ship escort and convoy operations in ice conditions. *Saf. Sci.* 95, 198–209. <https://doi.org/10.1016/j.ssci.2016.01.004>.

Haapala, J., Lönnroth, N., Stössel, A., 2005. A numerical study of open water formation in sea ice. *J. Geophys. Res.* 110.

Hänninen, S., 2004. Inventory List of Data Sources Available about Ship Hull Ice Loads and Damages, Report of Deliverable D2-1 of SafeIce Project. December 2004.

Kämäräinen, J., 1993. Evaluation of Ship Ice Resistance Calculation Methods. Helsinki University of Technology, A thesis for the degree of licentiate of technology.

Kotovirta, V., Jalonen, R., Axell, L., Riska, K., Berglund, R., 2009. A system for route optimization in ice-covered waters. *Cold Reg. Sci. Technol.* 55 (1), 52–62.

Kaupps, K., 2011. Modeling of the Ship Resistance in Compressive Ice. M.Sc. Thesis. Aalto University.

Kubat, I., 2012. Quantifying ice pressure conditions and predicting the risk of ship besetting. In: *Int. Conf. Exhib. Perform. Ships Struct. Ice 2012 (ICETECH 2012)*. Society of Naval Architects and Marine Engineers (SNAMe).

Kubat, I., Watson, D., Sayed, M., 2016. Ice compression risks to shipping over canadian arctic and sub-arctic zones. In: *Arctic Technology Conference*. <https://doi.org/10.4043/27348-ms>, 2016.

Külaots, R., Kujala, P., Von Bock Und Polach, R., Montewka, J., 2013. Modelling of ship resistance in compressive ice channels. In: *Proceedings of the International Conference on Port and Ocean Engineering under Arctic Conditions*. POAC (April 2014).

Kujala, P., Arughadhoss, S., 2012. Statistical analysis of ice crushing pressures on a ship's hull during hull-ice interaction. *Cold Reg. Sci. Technol.* 70, 1–11. <https://doi.org/10.1016/j.coldregions.2011.09.009>.

Kuuliala, L., Kujala, P., Suominen, M., Montewka, J., 2017. Estimating operability of ships in ridged ice fields. *Cold Reg. Sci. Technol.* <https://doi.org/10.1016/j.coldregions.2016.12.003>.

Last, P., Hering-Bertram, M., Linsen, L., 2015. How automatic identification system (AIS) antenna setup affects AIS signal quality. *Ocean Eng.* 100, 83–89. <https://doi.org/10.1016/j.oceaneng.2015.03.017>.

Lehtola, V., Montewka, J., Goerlandt, F., Guinness, R., Lensu, M., 2019. Finding safe and efficient shipping routes in ice-covered waters: a framework and a model. *Cold Reg. Sci. Technol.* 165 (June) <https://doi.org/10.1016/j.coldregions.2019.102795>.

Lehtiranta, J., Lensu, M., Haapala, J., 2012. Ice Model Validation on Local Scale. Finnish Meteorological Institute, Helsinki, Finland.

Lensu, M., Goerlandt, F., 2019. Big maritime data for the Baltic Sea with a focus on the winter navigation system. *Mar. Pol.* 104 (July 2018), 53–65. <https://doi.org/10.1016/j.marpol.2019.02.038>.

Li, F., Goerlandt, F., Kujala, P., Lehtiranta, J., Lensu, M., 2018. Evaluation of Selected State-Of-The-Art Methods for Ship Transit Simulation in Various Ice Conditions Based on Full-Scale Measurement. *Cold Regions Science and Technology*. <https://doi.org/10.1016/j.coldregions.2018.03.008>.

Li, F., Kujala, P., Montewka, J., 2019. A ship in compressive ice: an overview and preliminary analysis. In: *Proceedings of the International Conference on Port and Ocean Engineering under Arctic Conditions*. POAC, 2019-June(2009).

Lindqvist, G., 1989. A straightforward method for calculation of ice resistance of ships. In: *Proc. 10th Int. Conf. Port and Ocean Engineering under Arctic Conditions (POAC 1989)*. Luleå, Sweden.

Lu, L., Goerlandt, F., Valdez Banda, O.A., Kujala, P., Höglund, A., Arneborg, L., 2019. A Bayesian Network risk model for assessing oil spill recovery effectiveness in the ice-covered Northern Baltic Sea. *Mar. Pollut. Bull.* 139 (May 2018), 440–458. <https://doi.org/10.1016/j.marpolbul.2018.12.018>.

Lu, L., Goerlandt, F., Tabri, K., Höglund, A., Valdez Banda, O.A., Kujala, P., 2020. Critical aspects for collision induced oil spill response and recovery system in ice conditions: a model-based analysis. *J. Loss Prev. Process. Ind.* 66 <https://doi.org/10.1016/j.jlp.2020.104198>.

Mårtensson, S., Meier, H.E.M., Pemberton, P., Haapala, J., 2012. Ridged sea ice characteristics in the Arctic from a coupled multicategory sea ice model. *J. Geophys. Res.* 117, 1–16.

Montewka, J., Goerlandt, F., Kujala, P., Lensu, M., 2015. Towards probabilistic models for the prediction of a ship performance in dynamic ice. *Cold Reg. Sci. Technol.* 112, 14–28. <https://doi.org/10.1016/j.coldregions.2014.12.009>.

Montewka, J., Goerlandt, F., Lensu, M., Kuuliala, L., Guinness, R., 2019. Toward a hybrid model of ship performance in ice suitable for route planning purpose. *Proc. Inst. Mech. Eng. O J. Risk Reliab.* 233 (1), 18–34. <https://doi.org/10.1177/1748006X18764511>.

Newmark, J., 1959. A method of computation for structural dynamics. *Proceedings of the American Society of Civil Engineers* 85 (3), 67–94.

Riska, K., Kujala, P., Goldstein, R., Danilenko, V., Osipenko, N., 1995. Application of results from the research project 'A ship in compressive ice' to ship operability. In: *Proceedings of the International Conference on Port and Ocean Engineering under Arctic Conditions*. POAC, 1995-August(1995).

Riska, K., Wilhelmson, M., Englund, K., Leiviskä, T., 1997. Performance of merchant vessels in ice in the Baltic. In: *Tech. Rep. Report 52*. Winter Navigation Research Board, Helsinki.

Rosenblad, M., 2007. Increasing the Safety of Icebound Shipping – WP4 Operative Environment (Icebreaker Operations). Helsinki University of Technology, Espoo, Finland, 2007.

Saltelli, A., Chan, K., Scott, E.M., 2009. Sensitivity analysis. Wiley 2009.

Similä, M., Lensu, M., 2018. Estimating the speed of ice-going ships by integrating SAR imagery and ship data from an automatic identification system. *Rem. Sens.* 10 (7) <https://doi.org/10.3390/rs10071132>.

Su, B., Riska, K., Moan, T., 2010. A numerical method for the prediction of ship performance in level ice. *Cold Reg. Sci. Technol.* 60 (3), 177–188.

Uotila, J., 2001. Observed and modelled sea-ice drift response to wind forcing in the northern Baltic Sea. *Tellus, Series A: Dynamic Meteorology and Oceanography* 53 (1), 112–128. <https://doi.org/10.3402/tellusa.v53i1.12181>.

- Valdez Banda, O.A., Goerlandt, F., Kuzmin, V., Kujala, P., Montewka, J., 2016. Risk management model of winter navigation operations. *Mar. Pollut. Bull.* 108 (1–2), 242–262. <https://doi.org/10.1016/j.marpolbul.2016.03.071>.
- Vedenpää, L., 2011. The Second Field Campaign, Winter 2011. SAFEWIN Project Report.
- Wang, S., 2001. A Dynamic Model for Breaking Pattern of Level Ice by Conical Structures. D.Sc. Thesis. Helsinki University of Technology.
- Zhang, C., Zhang, D., Zhang, M., Mao, W., 2019. Data-driven ship energy efficiency analysis and optimization model for route planning in ice-covered Arctic waters. *Ocean Eng.* 186 (June), 106071. <https://doi.org/10.1016/j.oceaneng.2019.05.053>.
- Zhang, M., Zhang, D., Fu, S., Yan, X., Goncharov, V., 2017. Safety distance modeling for ship escort operations in Arctic ice-covered waters. *Ocean Eng.* 146 (October), 202–216. <https://doi.org/10.1016/j.oceaneng.2017.09.053>.
- Zhang, M., Zhang, D., Goerlandt, F., Yan, X., Kujala, P., 2019. Use of HFACS and fault tree model for collision risk factors analysis of icebreaker assistance in ice-covered waters. *Saf. Sci.* 111 (July 2018), 128–143. <https://doi.org/10.1016/j.ssci.2018.07.002>.
- Zhang, W., Goerlandt, F., Kujala, P., Qi, Y., 2018. A coupled kinematics model for icebreaker escort operations in ice-covered waters. *Ocean Eng.* 167 (August), 317–333. <https://doi.org/10.1016/j.oceaneng.2018.08.035>.
- Zhang, W., Zou, Z., Goerlandt, F., Qi, Y., Kujala, P., 2019. A multi-ship following model for icebreaker convoy operations in ice-covered waters. *Ocean Eng.* 180 (October 2018), 238–253. <https://doi.org/10.1016/j.oceaneng.2019.03.057>.